ISSN 0036-0295, Russian Metallurgy (Metally), Vol. 2019, No. 5, pp. 524–530. © Pleiades Publishing, Ltd., 2019.
Russian Text © The Author(s), 2019, published in Metally, 2019, No. 3, pp. 46–53.

Aging-Induced Hardening of Transition-Metal-Containing Al–Mg–Si Alloys Subjected to Deformation under Different Conditions

N. R. Bochvar[a], *, L. L. Rokhlin[a], I. E. Tarytina[a], and N. P. Leonova[a]

[a] *Institute of Metallurgy and Materials Science, Russian Academy of Sciences, Moscow, 119334 Russia*

**e-mail: bochvar@imet.ac.ru*

Received October 1, 2018; revised November 8, 2018; accepted November 8, 2018

Abstract—Metallographic analysis, hardness and electrical resistivity measurements, and tensile tests are used to study the behavior of Al–Mg_2Si alloys with (Sc + Zr) transition metal additions during aging performed after preliminary deformation under different conditions. It is shown that the decomposition of the supersaturated solid solution in the Al–Mg_2Si alloys with (Sc + Zr) transition metals and without them occurs in the same manner. However, the strength properties of the alloys with transition metals are higher than those of the alloys free from the transition metals because of substantial refining of solid-solution grains and a high density of dispersoid $(Sc_{1-x}Zr_x)Al_3$ aluminide particles. A peak hardness is observed for the alloys after quenching, equal channel angular pressing (ECAP), and aging. However, cold rolling after quenching before aging leads to an increase in the strength properties to a greater extent than ECAP performed under the same conditions.

Keywords: aluminum alloys, cold rolling, aging, strength properties, microstructure

DOI: 10.1134/S0036029519050045

INTRODUCTION

Alloys of the Al–Mg–Si system, the compositions of which are close to the pseudo-binary Al–Mg_2Si section, are among the precipitation-hardening alloys, which are hardened as a result of quenching and subsequent aging. At the stage of decomposition of the aluminum solid solution (which ensures almost a peak hardness), needlelike β"-phase crystals form, the crystal lattice of which is completely coherent with the matrix. At the next stage of decomposition, which is characterized by some softening after reaching the peak hardness, more coarse rods of the next β' phase form; at the final stage of decomposition, particles of the stable Mg_2Si phase form [1].

Combined scandium and zirconium additions to Al–Mg–Si alloys do not change the character of decomposition of the supersaturated aluminum solid solution as compared to that for the alloys free from transition metals but favor an increase in the recrystallization temperature and more fast hardening at the expense of precipitation of $(Sc_{1-x}Zr_x)Al_3$ aluminide particles from the solid solution [2]. However, the presence of scandium in Al–Mg–Si alloys can lead to a decrease in the hardening effect during artificial aging. The most probable explanation of the lesser hardening effect during aging of the studied alloys with transition metals (Sc or Sc + Zr) can be the fact that the metals refine aluminum solid solution grains. In this case, the amount of grain and subgrain boundaries in the alloys increases, which are preferable sites for the precipitation of particles formed upon the decomposition of the aluminum solid solution and being incoherent with it. Therefore, the amount of particles formed upon the decomposition of the aluminum solid solution, which are coherent with it, decreases, and the peak hardening of Al–Mg_2Si alloys during artificial aging is reached only at the expense of these particles. In contrast to artificial aging, natural aging of Al–Mg_2Si alloys with transition metals (Sc or Sc + Zr) leads to a certain increase in the hardness as a characteristic of the strength properties. This corresponds to the fact that the decomposition of the aluminum solid solution is independent of the presence of such additions (Sc or Sc + Zr) at this stage [3].

The application of severe plastic deformation (SPD), in particular, equal-channel angular pressing, leads to more active decomposition of the supersaturated solid solution along with the substantial grain refining in the aluminum solid solution and to the preparation of a material with high strength properties. The effect of SPD on the microstructure, the mechanical properties, and the precipitation of strengthening phases during aging of Al–Mg–Si alloys (series 6xxx) was studied in many works [4–9].

Table 1. Results of chemical analysis of the experimental Al-based alloys

Alloy	Content in alloy, %					Mg_2Si, %	Element excess, %	
	Si	Mg	Ti	Sc	Zr		Mg	Si
1	0.53	0.85	0.045	–	–	1.34	–	0.04
2	0.46	0.82	0.045	0.19	0.1	1.29	0.003	–

When studying the kinetics of precipitation of strengthening phases during aging after ECAP [4], it was shown that the precipitation of β'- and β"-phase particles depends on the number of passes; as the number of passes during ECAP increase, their precipitation occurs at a lower temperature. In this case, scandium-containing alloys exhibit higher stability of grains.

According to [5], as the number of passes during ECAP increases, the refining of initial grains in the structure of AA6063 alloy with a high degree of supersaturation leads to a substantial increase in the strength and plasticity.

The studies of the effect of ECAP and precipitation hardening on the mechanical properties of 6063 alloy (Al–Mg–Si) [6] showed that, after ECAP, the yield strength and the ultimate strength increase by 2 and 3 times, respectively. After natural aging, a microstructure and mechanical properties remain almost unchanged; however, after artificial aging at 180°C, the plasticity of the material increases and the hardening slightly decreases because of the annihilation of dislocations during heat treatment. It can be assumed that, individually, ECAP and aging improve some mechanical properties and degrade others; however a combination of the two processes unambiguously improves the strength properties of a material.

The evolution of the microstructure of an A6082 alloy (0.51% Si, 0.34% Mg) alloy with Zr and Zr + Sc additions after ECAP (route B_c, 8 passes) was described in [7]. The evolution of the microstructure of the alloy free from the additions depends on the presence of Mg_2Si and Si particles. The microstructure of the alloys with the additions (Zr and Zr + Sc) is stabilized by dispersoids. The hardening effect at the expense of Si particles in the completely annealed material is mainly due to the effect of Mg_2Si particles, whereas metastable β"-phase particles in the material subjected to SPD exhibit a widespread tendency to fragmentation; fine particles are more efficient within dislocations.

In [8], differential scanning calorimetry (DSC) was used to analyze the precipitation of phases during dynamic and static aging of Al–Mg–Si alloys, and the sequence of precipitation of strengthening β"- and β'-phase particles was revealed in accordance with the temperature of static and dynamic aging. The study of static aging at 191°C for 2, 4, and 10 h showed the presence of peaks corresponding to the β" and β'-phases at all temperatures. Dynamic aging was studied after solid-solution treatment and subsequent ECAP at 20, 110, 170, 191, and 300°C. DSC showed that, at room temperature and 300°C, the peaks of the β" and β' phases are absent in the DSC curves of samples subjected to ECAP; at 170 and 190°C, the β'-phase peaks are completely suppressed. These results confirm that the β" and β' phases were precipitated upon dynamic aging; in other words, during dynamic aging, the precipitates appear in samples after ECAP before DSC.

The effect of excess magnesium and silicon in the alloys corresponding to the pseudobinary section on the precipitation of disperse strengthening particles upon isothermal aging was studied in [9]. In the case of excess magnesium, after precipitation of β"-phase needles, β'-phase particle precipitate, which are in the form of rods; after that, plates of equilibrium β phase precipitate. In the case of excess silicon, platelike Si precipitates are present in the structure.

In the present work, the effect of different conditions of deformation and heat treatment before aging on the microstructure and the strength properties of Al–Mg–Si alloys with combined Sc + Zr additions is studied.

EXPERIMENTAL

The studies were performed using alloys prepared from high-purity metals (no less than 99.8% purity).[1] The magnesium and silicon contents in the alloys were taken to be close to those corresponding to the pseudobinary Al–Mg_2Si section; the content of Mg_2Si in the alloys was ~1.4%. The alloys are based on aluminum. The contents of other elements (%) are 0.8 Mg, 0.46 Si, and 0.05 Ti; additionally, the alloys contain 0.2% Sc and 0.15% Zr. Table 1 shows results of chemical analysis performed by atomic emission spectroscopy using inductively coupled plasma. According to the data, the compositions of the alloys agree adequately with the charge compositions. The content of Mg_2Si is ~1.3%; there is a slight silicon excess in the alloy free from (Sc + Zr) additions. Thus, the compositions of the alloys almost correspond to the pseudobinary Al–Mg_2Si section.

The alloys for investigation were prepared using an electric resistor furnace and a graphite–chamotte crucible. Silicon and transition metals were made a part of

[1] From here on, the compositions are given in wt %.

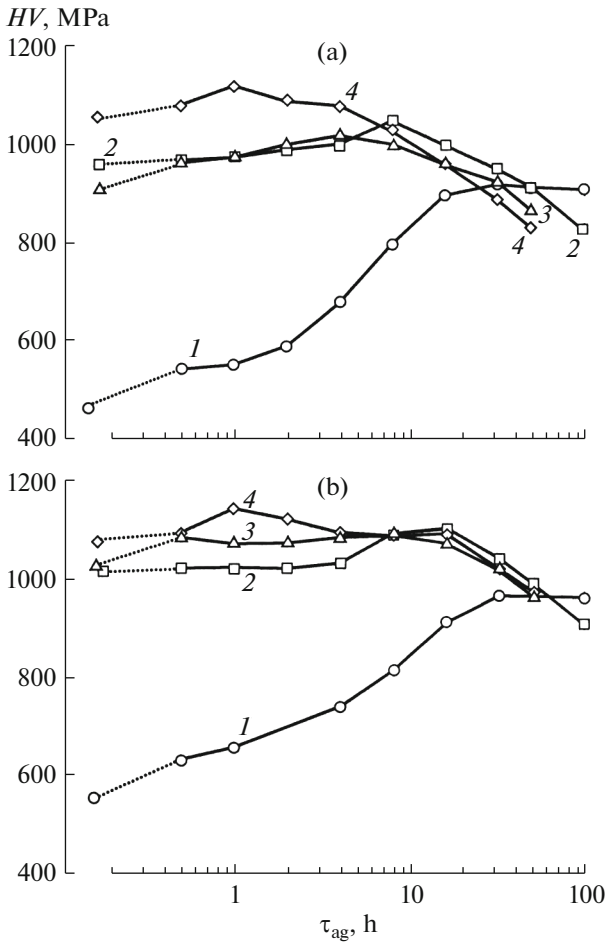

Fig. 1. Variations of the hardness of (a) Al–Mg_2Si and (b) (Sc + Zr)-containing Al–Mg_2Si alloys subjected to different treatments and subsequently aged at 170°C for different times τ_{ag}: (*1*) quenching, (*2*) cold rolling, (*3*) quenching + cold rolling, and (*4*) quenching + ECAP.

the melt using preliminary prepared master alloys; magnesium was made a part of the melt using the pure metal. The alloys were cast into a steel three-hole mold at ~720°C; the diameter and the height of each hole were 25 and 120 mm, respectively. After casting and turning of ingots to a diameter of 20 mm, they were subjected to homogenizing annealing at 480°C for 4 h. One of the ingots of each composition was subjected to cold rolling to form rods 8 × 8 mm in section (drawing ratio was $\mu = 4.9$). Half the rod was retained in the cold-rolled state; the other half and two other ingots of each composition were heated to 525°C, held for 2 h, and subjected to water quenching at room temperature. To prevent natural aging, the quenched ingots were stabilized at 150°C for 20 min. After quenching and stabilization, the ingots were subjected to either cold rolling ($\mu = 4.9$) or ECAP using 6 passes, 120° channel intersection angle, and B_c route, i.e., after each pass, the ingot was rotated about its longitudinal axis through an angle of 90°. The true strain was $\varepsilon = 5.4$. After the aforementioned treatments, the rods were subjected to aging at 170°C for 0.5 to 100 h.

The samples were studied using hardness and electrical resistivity measurements, mechanical tests, and metallographic analysis. The Brinell hardness was measured at a load of 625 N by the indentation of a ball 2.5 mm in diameter using an IT-5010-01M tester equipped with an electronic calculation system. The electrical resistivity of the alloys was measured using a BSZ-010-2 microhmmeter and cylindrical samples having a gage length of 27.5 mm and a diameter of 6 mm. Sections for metallographic studies were prepared by grinding using abrasive papers with progressively decreasing abrasive particle sizes and subsequent polishing using a cloth and a water suspension of chromium oxide; final etching was performed using Keller's reagent, which is an aqueous solution of nitric (2.5 cm^3), hydrochloric (1.5 cm^3), and hydrofluoric (0.5 cm^3) acids.

Polarized light microscopy was performed using sections first subjected to electrolytic polishing in an electrolyte consisting of 400 mL orthophosphoric acid (the density is 1.54 g/cm^3), 100 mL sulfuric acid (the density is 1.84 g/cm^3), 50 g chromium anhydride, and 25 mL water. The heating temperature of the electrolyte was 70–90°C; the voltage and current density were 15–20 V and 0.8 A/cm^3, respectively. Electrolytic polishing was carried out for 1–3 min. After that, the section surface was oxidized at room temperature for 3 min using a 1.8% aqueous solution of HBF_4, a voltage of 13 V, and a current of ~1 A.

The mechanical properties were studied by tensile tests on samples 3 mm in diameter, which were cut along the longitudinal axis; the tests were conducted at a tensile rate of ~1 mm/s using an Instron-3382 machine.

RESULTS

Figures 1a and 1b show the hardness of the Al–Mg_2Si alloys without and with transition metals, which were subjected to various treatments, as functions of the time of artificial aging at 170°C. It is seen that the hardness of the alloys with Sc + Zr (see Fig. 1b) is higher than that of the unalloyed (with the transitions metals) Al–Mg_2Si alloys (see Fig. 1a). In both cases, the alloys subjected to ECAP (after quenching) exhibit peak properties (Fig. 1, curves *4*). The alloys subjected to quenching and subsequent aging (without intermediate deformation) exhibit the lowest hardness (see Fig. 1, curves *1*). However, after reaching a peak hardness on 16-h aging, the alloys retain an unchanged hardness upon aging for 100 h, whereas the alloys subjected to treatment under other conditions begin to loss the hardness after reaching a peak hardness upon aging for 8–16 h. This is especially true of the alloys subjected to ECAP. Data on the

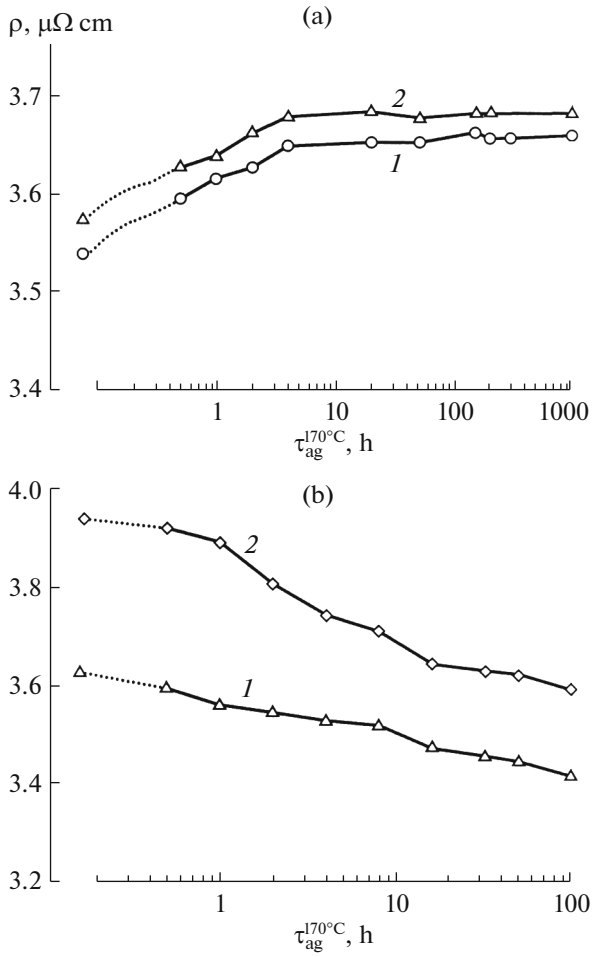

Fig. 2. Variations of the electrical resistivity of (*1*) Al–Mg_2Si and (*2*) (Sc + Zr)-containing Al–Mg_2Si alloys during (a) natural aging and (b) artificial aging at 170°C.

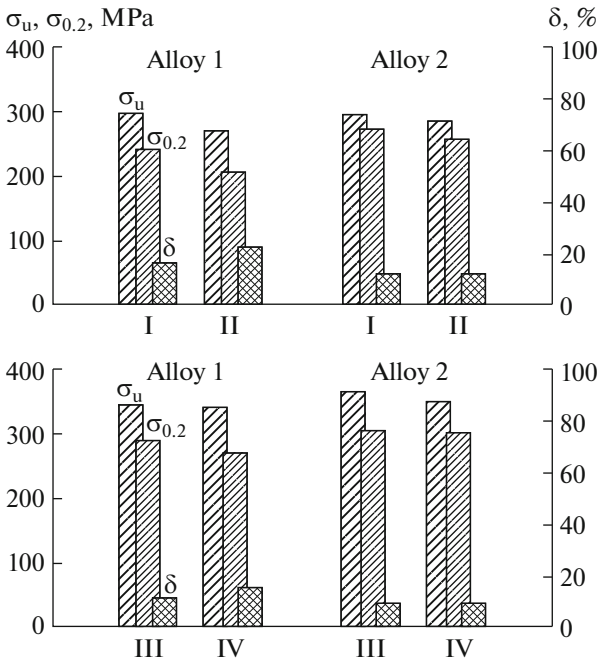

Fig. 3. Mechanical properties of alloys 1 and 2 after treatment under different conditions: (I) cold rolling + aging at 170°C for 8 h, (II) quenching + aging at 170°C for 16 h, (III) quenching + cold rolling + aging at 170°C for 8 h, and (IV) quenching + ECAP + aging at 170°C for 1 h.

electrical resistivity of the quenched alloys subjected to natural (Fig. 2a) and artificial (Fig. 2b) aging indicate the decomposition of the supersaturated solid solution.

Figure 3 shows the results of tensile tests of alloys 1 and 2 (see Table 1) subjected to different treatments. Preliminary, the samples were annealed at 170°C for the time that ensures reaching the peak hardness in accordance with the data in Fig. 1. After cold rolling and annealing at 170°C, the unalloyed compositions and compositions alloyed with (Sc + Zr) exhibit higher strength properties (regimes I and III) as compared to those of the quenched and subsequently aged alloys (regime II).

The microstructure of the alloys in different states was studied (Figs. 4, 5). The structure of the cast alloys (Fig. 4a) consists of the Al-based solid solution dendrites; the second phases in the form of Mg_2Si magnesium silicide particles and (Sc, Zr)Al_3 transition metal aluminides are observed between dendrite arms. After homogenizing annealing at 480°C for 4 h, second phases are partially dissolved in the aluminum solid solution; a small amount of undissolved second phases is observed along grain boundaries and within solid solution grains (Fig. 4b). After cold rolling (Fig. 4c), grains and second-phase precipitates are located along the rolling direction; after ECAP (Fig. 4d), the structure of the alloys in the longitudinal direction is a random mixture of refined grains characterized by fragmentation.

The microstructure of the alloys is most visible in studying with polarized light (see Fig. 5). Figures 5a, 5b show the microstructure of the alloys quenched after heating to 525°C. It is seen that the combined (Sc + Zr) additions favor substantial solid-solution grain refining. Cold rolling performed after quenching leads to the formation of the structure characterized by grains elongated along the rolling direction (Figs. 5c, 5d); the compositions alloyed with the transition metals are characterized by finer grains (see Fig. 5d). The microstructure of the quenched alloys subjected to ECAP, in the center of ingot and at the longitudinal edge (Figs. 5e, 5f), indicates a substantial crystal lattice distortion of aluminum solid solution grains.

DISCUSSION

An analysis of the dependence of the electrical resistivity of the alloys on the time of aging at 20°C allows us to conclude that, during natural aging, the

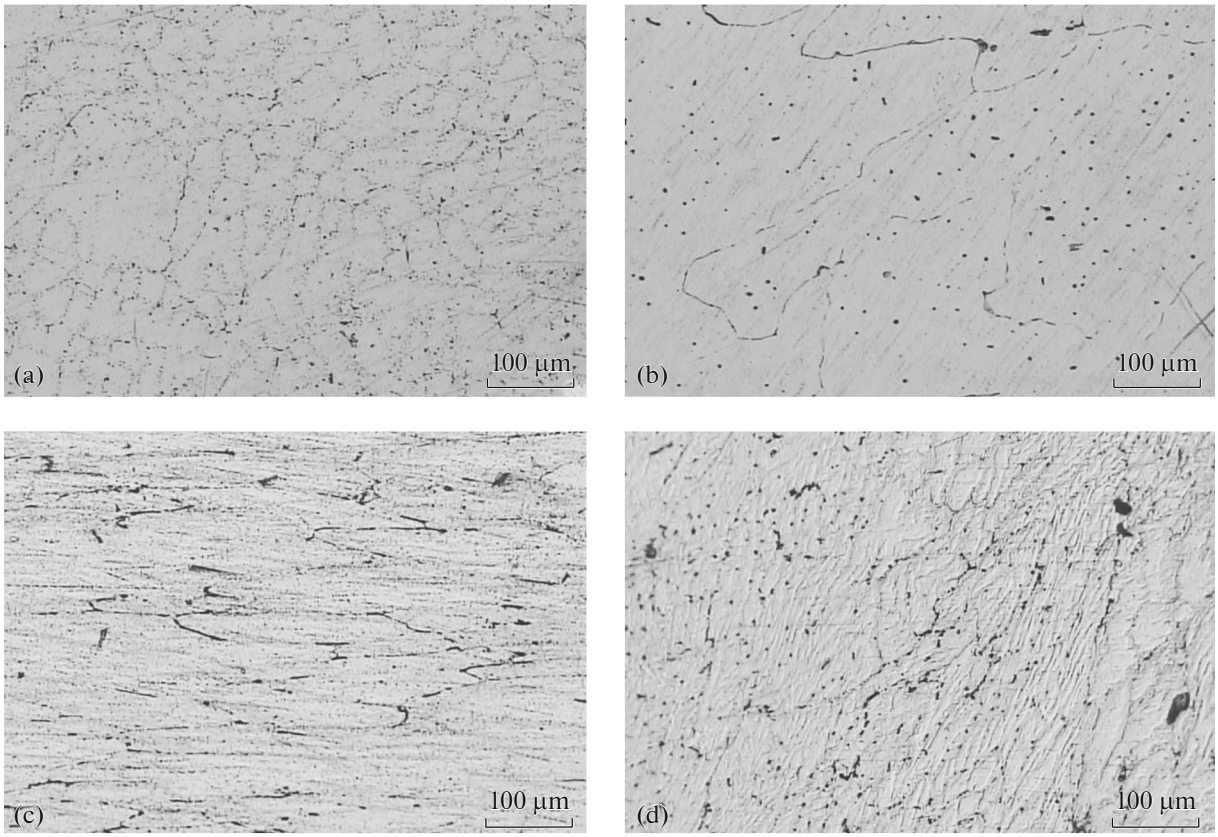

Fig. 4. Microstructure of (a, b) Al–Mg_2Si and (c, d) (Sc + Zr)-containing Al–Mg_2Si alloys in different states: (a) cast, (b) homogenized, (c) cold-rolled, and (d) after ECAP.

electrical resistivity progressively increases up to $\tau_{ag}^{20^\circ C} = 8$ h and, after that, becomes almost unchanged (see Fig. 2a). According to data of [10], the formation of metastable β"-phase particles takes place, which are coherent with the matrix. The subsequent artificial aging at 170°C (see Fig. 2b), which was performed directly after quenching, demonstrates a decrease in the electrical resistivity up to $\tau_{ag}^{170^\circ C} = 8$ h; then, the rate of decrease in the electrical resistivity decreases and, after 16-h aging, varies insignificantly. The electrical resistivity of the alloys with (Sc + Zr) additions (see Fig. 2b, curve *2*) decreases more actively and the decrease becomes slower after 16-h aging. The associated variations of the hardness of the alloys without additions and with (Sc + Zr) additions (see curves *1* in Figs. 1a, 1b) show that, as the aging time increases, the hardness increases and reaches an unchanged value at $\tau_{ag} = 16$ h; this corresponds to the change in the electrical resistivity given in Fig. 2b. Reaching the peak hardness is related to the precipitation of needle-like β"-phase crystals in the aluminum solid solution; the crystal lattice of the phase is completely coherent with the matrix.

The higher hardness and electrical resistivity of the alloys with the (Sc + Zr) addition are related to the substantial refining of solid solution grains after quenching (see Figs. 5a, 5b) and a high density of $(Sc_{1-x}Zr_x)Al_3$ dispersoids. Electron-microscopic studies of the alloys subjected to quenching and aging at 170°C for 16 and 50 h, which were performed previously [3], showed the presence of a great amount of dispersoids in the alloy structure and the appearance of the metastable β' phase in the structure of overaged alloy. The dispersoids are $(Sc_{1-x}Zr_x)Al_3$ aluminide precipitates surrounded by elastic deformation in the form of dark half moons; the spherical precipitates are between the half moons [11]. The presence of these dispersoids favors higher strength characteristics of the alloys containing scandium and zirconium.

The quenched alloys subjected to cold rolling or ECAP and alloys subjected to rolling after homogenizing annealing without quenching exhibit another behavior during aging. As is seen from Fig. 1 (curves *2–4*), the hardness of the alloys corresponds to the hardness of the deformed metal. For the alloys free from transition metals, a slight increase in the hardness is observed in the case of the following regimes of treatment: quenching + ECAP and 1-h aging (curves *4*), quench-

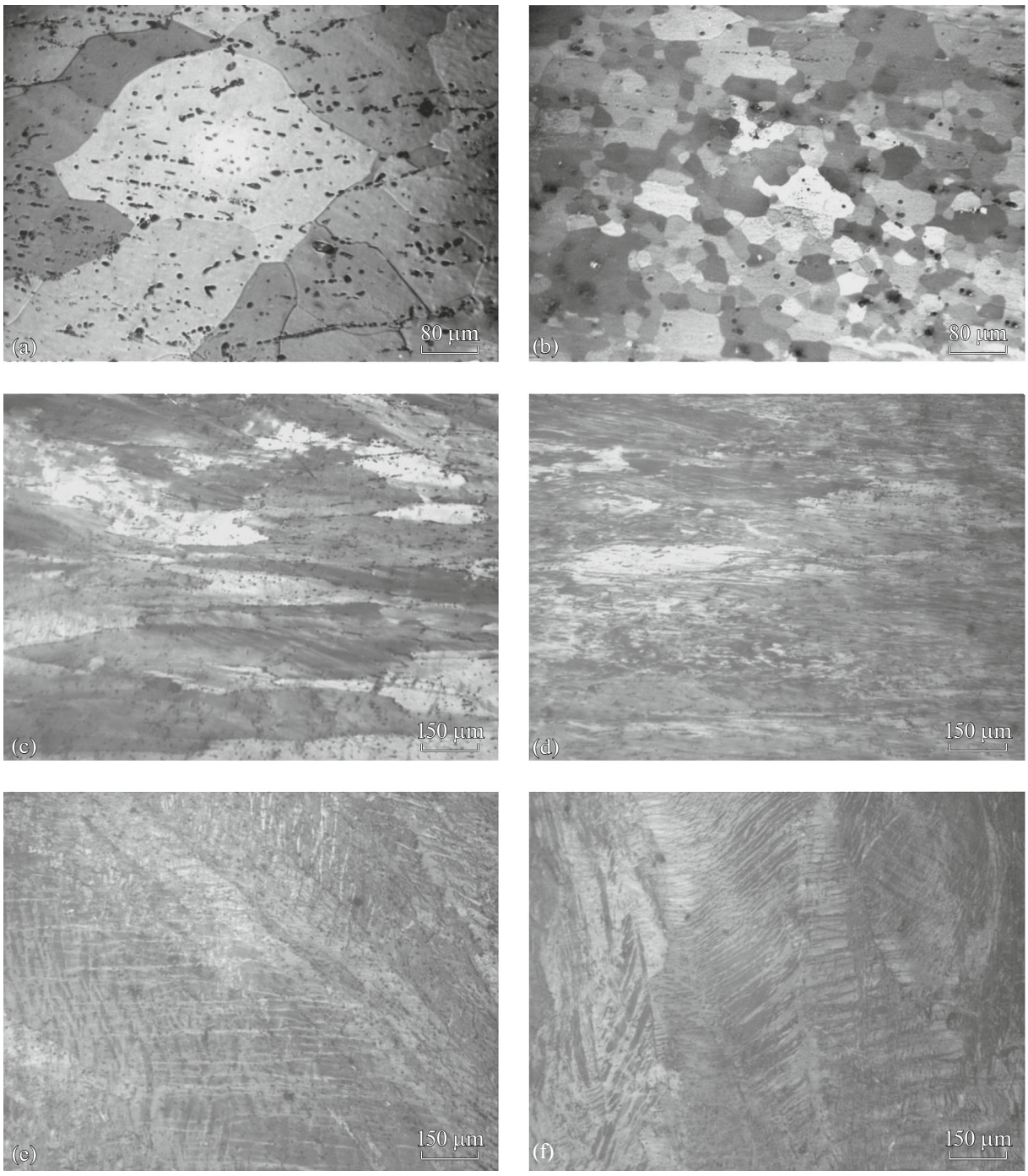

Fig. 5. Microstructure (polarized light) of (a, c) Al–Mg_2Si and (b, d–f) (Sc + Zr)-containing Al–Mg_2Si alloys (along the rolling direction) in different states: (a, b) after quenching, (c, d) after quenching and cold rolling, and (e, f) after quenching and ECAP (edge and center of sample, respectively).

ing + cold rolling and 4-h aging (curves *3*), and cold rolling without preliminary quenching and 8-h aging (curves *2*). It is seen that, after slight increase in the hardness, softening takes place. Softening of the alloys with (Sc + Zr) takes place after slightly more prolonged holdings. The fact that the alloys are weakly aged is related to large lattice distortions of the aluminum solid solution during cold rolling and ECAP, an increase in the density of dislocations, and a high amount of metastable phases precipitated within solid solution grains and at their boundaries. The strengthening β" and β' phases precipitated during deformation prevent the motion of dislocations and, therefore, softening to a greater extent as compared to the effect

of the dispersed phases precipitated from the solid solution during subsequent aging. Images of the microstructure show the existence of a great amount of dispersed phases along boundaries of deformed grains (see Figs. 4c, 4d) and substantial oblongness of grains along the rolling direction (see Figs. 5c, 5d). A more substantial crystal lattice distortion is observed after ECAP (see Figs. 5e, 5f).

The results of the analysis of the obtained data on the strength properties of alloys 1 (Al–Mg_2Si) and 2 (Al–Mg_2Si alloyed with (Sc + Zr)) are as follows. The alloys subjected to cold rolling after preliminary quenching (see Fig. 3, III) have peak strength properties as compared to those of the alloys cold-rolled without preliminary quenching (see Fig. 3, I) and the quenched alloys that were not subjected to deformation (Fig. 3, II). The difference in the yield strengths of alloys 1 is 50 and 76 MPa, whereas that for alloys 2 it is 72 and 81 MPa, respectively. A comparison of the strength properties of the alloys subjected to quenching followed by cold rolling (see Fig. 3, III) or ECAP (see Fig. 3, IV) shows that alloys 2 with (Sc + Zr) exhibit higher strength yields as compared to those of alloys 1 free from the transition metals; the difference is 16 and 4 MPa, respectively. After aging, peak strength properties are observed for the alloys subjected to cold rolling after preliminary quenching; the lowest strength is observed for the alloys subjected to aging after preliminary quenching. When comparing the hardness and yield strength of alloy 1 (free from transition metals) subjected to quenching + ECAP + aging at 170°C (see Fig. 1a, curve *4*) and quenching + cold rolling + aging at 170°C (curve *3*), it can be seen that the samples subjected to quenching + ECAP + aging at 170°C (see Fig. 1a, curve *4*) exhibit a higher strength as compared to that of the samples subjected to quenching + cold rolling + aging at 170°C (see Fig. 3, I).

Analogous behavior is observed for the samples of alloy 2 alloyed with (Sc + Zr) transition metals. The samples subjected to quenching + ECAP + aging at 170°C (see Fig. 1b, curve *4*) exhibit a higher hardness; the samples subjected to quenching + cold rolling + aging at 170°C (see Fig. 3, III) exhibit a higher strength. Thus, we can conclude that cold rolling at a drawing ratio $\mu \sim 4.9$ is a more efficient process for reaching high properties of the material as compared to ECAP.

CONCLUSIONS

(1) The effect of different treatment conditions on the structure, the precipitation hardening, and the strength properties of Al–Mg_2Si alloys and Al–Mg_2Si alloys with combined (Sc + Zr) additions was studied. It is shown that cold deformation suppresses the precipitation of metastable phases from the solid solution during aging at 170°C in the alloys without and with a combined (Sc + Zr) transition metal addition.

(2) It was found that a peak ultimate strength and yield strength are reached for the alloys subjected to cold plastic deformation (drawing ratio is $\mu \sim 4.9$) after preliminary quenching, whereas a peak hardness is observed for the alloys subjected to ECAP ($\varepsilon = 5.4$).

FUNDING

This study was performed in terms of state assignment no. 007-00129-18-00.

REFERENCES

1. G. Thomas, "The ageing characteristics of aluminum alloys," J. Inst. Met. **90**, 57–63 (1961–1962).
2. V. G. Davydov, V. I. Elagin, V. V. Zakharov, and T. D. Rostova, "On alloying of aluminum alloys with scandium and zirconium," Metalloved. Term. Obrab. Met., No. 8, 25–30 (1996).
3. L. L. Rokhlin, N. R. Bochvar, N. Yu. Tabachkova, and A. V. Sukhanov, "Effect of scandium on the kinetics and hardening of Al–Mg_2Si alloys," Tekhnol. Legkikh Splavov, No. 2, 53–62 (2015).
4. M. Vedani, G. Angella, P. Bassani, D. Ripamonti, and A. Tuissi, "DSC analysis of strengthening precipitates in ultrafine Al–Mg–Si alloys," Therm. Analys. Calorimetry **87** (1), 277–284 (2007).
5. M. Samaee, S. Najafi, A. R. Eivani, H. R. Jafarian, and J. Zhou, "Simultaneous improvements of the strength and ductility of fine-grained AA6063 alloy with increasing number of ECAP passes," Mater. Sci. Eng. A **669**, 350–357 (2016).
6. B. Mirzakhani and Y. Payanden, "Combination of severe plastic deformation and precipitation hardening processes affecting the mechanical properties in Al–Mg–Si alloy," Mater. Design. **68**, 127–133 (2015).
7. M. Cabibbo, C. Scalabroooni, and E. Evangelista, "Effects of severe plastic deformation induced by equal-channel angular pressing in the AA1200, AA5754, AA6082 and AA6106 modified with Zr and Zr + Sc," Met. Sci. Technol. **24** (1), 31–40 (2013).
8. M. Liu, Z. Wu, R. Yang, J. Wei, Y. Yu, P. C. Skaset, and H. J. Roven, "DSC analysis of static and dynamic precipitation of an Al–Mg–Si–Cu aluminum alloy," Prog. Nat. Sci.: Mater. Intern. **25**, 153–158 (2015).
9. L. C. Doan, K. Nakai, J. Matsuura, S. Kobayashi, and Y. Ohmori, "Effects of excess Mg and Si on the isothermal ageing behaviour in the Al–Mg_2Si alloys," Mater. Trans. **43** (6), 1371–1380 (2002).
10. T. V. Shchegoleva, "Aging mechanism of an Al–Mg–Si alloy," Fiz. Met. Metalloved. **25** (2), 246–254 (1968).
11. M. E. Drits, L. B. Ber, Yu. G. Bykov, L. S. Toropova, and G. N. Anastas'eva, "Aging of the Al–0.3 at % Sc alloy," Fiz. Met. Metalloved. **57** (6), 1172–1179 (1984).

Translated by N. Kolchugina